frontiers in Sustainability

ORIGINAL RESEARCH
published: 16 July 2021
doi: 10.3389/frsus.2021.697265

Upcycling of Wastewater Sludge Incineration Ash as a 3D Printing Technology Resource

Dongwon Ki[1], Shin Young Kang[1] and Kwang-Min Park[2]*

[1] Division of Living and Built Environment Research, Seoul Institute of Technology, Seoul, South Korea, [2] Construction Technology Research Center, Korea Conformity Laboratories, Seoul, South Korea

Recycling of usable resources from waste must be prioritized to adhere to the circular economy policy implemented worldwide. This study aims to use wastewater sludge incineration ash (WSIA), which is a by-product of wastewater sludge treatment processes, in the 3D printing industry as a sustainable material. First, we explored the stability of incinerated ash generated from a wastewater treatment facility in Seoul by evaluating its physical (water content, organic matter content, and particle size) and chemical (oxide compound composition) characteristics. Composition ratios of the predominant oxides of silicon (SiO_2), aluminum (Al_2O_3), phosphorous (P_2O_5), iron (Fe_2O_3), and calcium (CaO) were stable for 6 months. This finding indicates the potential for the incinerated ash to be commercially viable as a powder-bed 3D printed geopolymer. We then examined the optimal ratio of admixtures between the incinerated ash and ultrarapid hardening cement and the following post-treatment process method as a curing stage. The composite material made with 25% WSIA exhibited stability during the curing stage using alkaline solutions, and its compressive strength and water absorption were in accordance with the values recommended by the Korean Standard for decorative concrete blocks (KS F 4038). Additionally, a geopolymer prototype with 25% incinerated ash was produced. To support efficient upcycling of WSIA, long-term environmental and functional monitoring of the final product, effects of incinerated ash particle sizes, and post-treatment process times were further investigated to reduce costs.

Keywords: waste recycling, construction application, powder-based 3D printing, sewage sludge ash, waste-to-resource

OPEN ACCESS

Edited by:
Davide Settembre Blundo, Rey Juan Carlos University, Spain

Reviewed by:
Alexandros Maziotis, Pontificia Universidad Católica de Chile, Chile
Taha A. El-Sayed, Benha University, Egypt

****Correspondence:***
Dongwon Ki
dongwonk@sit.re.kr

Specialty section:
This article was submitted to Circular Economy, a section of the journal Frontiers in Sustainability

Received: *19 April 2021*
Accepted: *14 June 2021*
Published: *16 July 2021*

Citation:
Ki D, Kang SY and Park K-M (2021) Upcycling of Wastewater Sludge Incineration Ash as a 3D Printing Technology Resource. Front. Sustain. 2:697265. doi: 10.3389/frsus.2021.697265

INTRODUCTION

Utilizing waste as raw materials for manufacturing new products leads to material circularity, which helps in shifting the conventional take–make–dispose linear material flow economic model to a circular economic model. There is debate surrounding the definition, limitation, and assessment of the circular economy, which is gaining attention from all sectors of academia, industry, and local and national administrations. Policy changes and development of waste-based materials within the closed loop of production, consumption, management, and recycling can promote minimizing the use of virgin materials and waste generation and improve energy efficiency (Murray et al., 2017; Mayer et al., 2019; Guerra-Rodríguez et al., 2020; Salmenperä et al., 2021). To shift toward a true circular economy, many countries are establishing waste-based material policies with

long-term sustainability concepts, thus contributing to climate neutrality (EU, 2020; Salmenperä et al., 2021). Waste utilization is also in line with the UN Sustainable Development Goal 12 (SDG 12: "Responsible Consumption and Production"), which promotes the reduction, reuse, and recycling of wastes and the efficient management of natural resources (UN, 2016).

Wastewater sludge or sewage sludge is a by-product of wastewater treatment processes. The mixture of organics and inorganics in wastewater sludge should be properly treated or recovered as downstream resources (Guerra-Rodríguez et al., 2020). Energy from thickened sludge is recovered biologically through anaerobic digestion, and nutrients, such as phosphorous and nitrogen, are recovered for use as fertilizers (struvite, ammonium sulfate or nitrate, and calcium phosphate) (Burton et al., 2014; Cieślik and Konieczka, 2017). In addition to the resources extracted from wastewater sludge, an ash end product is produced after drying, carbonization, composting, or incineration, depending on the process employed by the wastewater treatment facility. The ash end product is a by-product of the treatment but can also be used as a resource (Lynn et al., 2016; Rezaee et al., 2019). Physical and biochemical treatment processes, such as drying, carbonization, and composting, result in varying organic content levels in the ash and can be applied as a heat energy source for a thermal power plant or as a compost for land application (Epstein et al., 1976; Park and Jang, 2011; Bianchini et al., 2015). The incineration by-product provides various advantages, such as (i) significant sludge volume reduction, (ii) thermal/toxic compound destruction, (iii) heat recovery during the process, and (iv) minimal residual odor issues. These advantages result in more efficient waste management and application as a construction material, i.e., aggregates, concrete mixture, and asphalt paving mixtures (Tantawy et al., 2012). Drying and incineration are the treatment methods for wastewater sludge in Seoul, South Korea. The cost of producing incinerated ash in Seoul was ∼$70 per ton in 2020. However, to support circular and efficient material use, we should investigate maintaining profits while utilizing raw materials and reducing waste. In South Korea, wastewater sludge as well as sludge-derived by-products, such as ash, have been categorized as "industrial wastes," thereby implying that the drying and incineration ashes cannot be freely extracted, delivered, and used without obtaining permission. Since the Framework Act on Resources Circulation was enacted in 2016 to move toward a sustainable resource-circulating society, a new "Circular Resources Accreditation System" has been in effect to support the use of wastes as resources by excluding them from waste-related regulations (Lee and Kang, 2016). To utilize the system more efficiently, new value-adding options for the waste should be proposed and included in the business model.

This study focuses on exploring the use of wastewater sludge incineration ash (WSIA) as a possible material for 3D printing, particularly for construction applications. Three-dimensional printing is an additive manufacturing technology and is one of the Fourth Industrial Revolution technologies (Maynard, 2015). The application of 3D printing technology in construction has recently gained attention and experienced rapid development, owing to the availability of automated production processes that minimize construction time and labor (Lim et al., 2012; Wu et al., 2016; Nematollahi et al., 2017). As a component of 3D printing materials, WSIA could be used in construction applications. It is particularly suitable for applications using powder-based inorganic materials by employing the methods of material extrusion, including fused deposition modeling, and binder jetting (BJ) among seven 3D printing methods (ASTM International, 2015). Ordinary Portland cement (OPC) is traditionally used in the construction industry; however, in recent years, several sustainable BJ 3D printing alternatives have been studied to replace OPC, which exhibits a high energy demand and produces carbon dioxide (Xia and Sanjayan, 2016, 2018; Nematollahi et al., 2017, 2019; Park et al., 2018; Xia et al., 2019). Alternatives include an inorganic polymer or geopolymer, which acts as the binding agent in concrete via geopolymerization reactions (Davidovits, 1989). In previous studies, print quality, depositability, and wettability were estimated for an OPC alternative powder that contained a mixture of ball-milled anhydrous-Na_2SiO_3, slag, and fine sand. Studies also show that additional post-treatment for 3D printed products results in a compressive strength that is ∼18 times greater than that observed before post-treatment (Xia and Sanjayan, 2016). Moreover, to improve geopolymer strength, diverse processing conditions, such as curing temperature, medium, and time during post-processing were assessed along with different mixing proportions of geopolymer precursors (Park et al., 2018; Xia and Sanjayan, 2018; Nematollahi et al., 2019; Xia et al., 2019). The development of sustainable 3D printed alternatives to OPC is still in the early stages of commercialization or application in the construction industry.

In this study, we successfully prepared a new composite material by mixing WSIA with commercially available cement, thus demonstrating the importance of WSIA. No previous studies have used WSIA as a potential material in 3D printing. We first confirmed the stability of the physical and chemical characteristics of WSIA generated from a wastewater treatment facility belonging to the Seoul Metropolitan Government of South Korea. Next, the optimal mixing ratios of the ash to the commercial cement and postprocessing medium were evaluated. The study results present an innovative application of a value-added waste resource as a 3D printing technology material. Furthermore, we put forward the current limitations related to policy implications and discuss the circular economy and environmental sustainability when WSIA is used as a resource.

MATERIALS AND METHODS

System Description for 3D Printing Application Using WSIA

Figure 1 simplifies the process of wastewater sludge becoming a 3D printed final product, including incineration, mixing commercial cement and WSIA, 3D printing, and post-treatment. Detailed methods and materials for this study are described in the following sections.

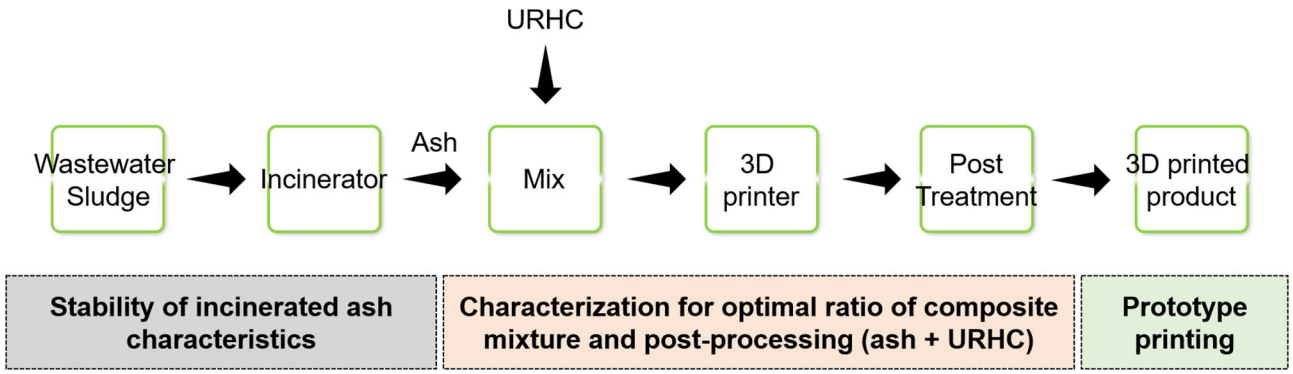

FIGURE 1 | Simplified flow diagram for 3D printing application when using WSIA. URHC is a commercial material used in 3D printing.

TABLE 1 | List of post-treatment options tested, including solution pH and preparations.

Experiment	Post-treatment condition	pH	Preparation
1	Without post-treatment	-	-
2	Water	∼7	Tap water
3	Sodium silicate (Na_2SiO_3) solution	∼11	Purchased
4	Sodium silicate (Na_2SiO_3) solution + NaOH, Na_2SiO_3/NaOH = 0.95	11–12	Lab prepared
5	Polydimethylsiloxane (PDMS)	8.2–9	Lab prepared

Wastewater Sludge Incineration Ash (WSIA)

In this study, wastewater sludge is defined as dewatered sludge cakes. In Seoul, there are four wastewater treatment plants (J, N, S, and T) with drying and incineration facilities; all plants have drying facilities, and N and S plants also comprise incineration facilities. The total production of wastewater sludge in Seoul was 1938 t/day in 2019 as reported by the most recent Korean national statistics (Ministry of Environment, 2020). In this study, we used WSIA sampled from the N wastewater treatment plant, which includes a fluidized bed incinerator. In 2019, the plant processed 142 t/day of wastewater sludge for incineration and produced 12 t/day of WSIA after incineration. Bottom and fly ash are produced during the incineration process. Bottom ash contents (1%) are negligible compared with those of fly ash (99%); thus, the WSIA is considered to be composed of fly ash.

The WSIA was collected monthly from plant N from May to October 2020. Physical and chemical properties of the ash were measured, including particle size, water content, organic matter content (or ignition loss), and oxide compound concentrations. The particle size distribution ranged from 0.017 μm to 2 mm and was measured using an LS 13 320 particle size analyzer (Beckman Coulter Inc., USA) and laser diffraction methods (ISO 133209:2020). Water and organic matter content were determined according to the Korean Official Wastes Test Method (Ministry of Environment (MOE), 2017). Oxide compounds were analyzed using inductively coupled plasma-optical emission spectroscopy (ICP-OES, Optima 8300, PerkinElmer, UK). Rietveld profiles derived from powder X-ray diffraction (PXRD, MINIFLEX 600, Rigaku, Japan) were analyzed to characterize crystalline structures in WSIA for the samples from May and August 2020.

Binder Jetting 3D Printing Process

The WSIA was blended with a commercially available ultrarapid hardening cement (URHC, Unijet cement, UNION Corp., Seoul, South Korea) to produce a composite and printable powder using a mortar mixer (10 L volume) for 10 min. Then, the WSIA was added in different weight ratios: 0, 25, and 50%. Detailed physical properties of URHC, as reported by the supplier, are included in the **Supplementary Material**. The composite dry mix with ash and URHC was loaded into the powder print bed of a binder-jetting 3D printer (BJ3DP, ProJet CJP 360) manufactured by 3D SYSTEMS (Rock Hill, SC, USA). SketchUp (Trimble Inc., Sunnyvale, CA), which is a 3D design and modeling computer-aided design program, was then used to create two digital models of a cubic specimen and a prototype plate. Additive manufacturing procedures for the BJ3DP are provided in the **Supplementary Material**. The zb® 63 binder (3D SYSTEMS, Rock Hill, SC, USA), which includes 0–1% 2-pyrrolidone in distilled water (Asadi-Eydivand et al., 2016), is commercially available and has been used as an adhesive liquid for the BJ3DP. The printing layer thickness was fixed at 0.1 mm. After the printing process, the designed cubic specimen (∼20 × 20 × 20 mm) and a prototype (∼200 × 80 × 20 mm) were depowdered using an air compressor to remove excess powder. Then, the cube specimen and prototype were post-treated with a curing medium solution to elucidate important mechanical properties such as strength. A control that did not undergo any post-treatment and the different post-processing conditions that were tested (Experiments 1–5) are summarized in **Table 1**. Sodium silicate solutions were tested in Experiments 3 and 4. For Experiment 3,

Sikafloor® CureHard-24 (Sika Limited, Hertfordshire, UK) was purchased and used; for Experiment 4, a lab-prepared solution with a liquid-type sodium silicate solution (SiO_2 28.2%, Na_2O 9.3%, H_2O 65.5%, Na_2SiO_3, 1M) and sodium hydroxide (NaOH, 3M) was used. A post-treatment solution of polydimethylsiloxane (PDMS) was prepared in the lab and used in Experiment 5. This coating material is used to reduce the water permeability in concrete, and it is cost-effective, non-toxic, non-flammable, and non-volatile (Wang et al., 2020). The PDMS properties used in this study are described in a previous study (Lee et al., 2017).

Based on the cubic specimen tests, we printed a prototype plate structure by employing the same 3D printer that is used for the cubic samples with the most effective mixing ratio of WSIA and URHC. Considering the capacity of the 3D printer, ~200 additive layers were built for the prototype, and the detailed procedures are provided in the **Supplementary Materials**.

Mechanical and Environmental Specimen Evaluation

Mechanical parameters of dry bulk density (ρ_{bulk}, g/cm^3), water absorption rate (%), and compressive strength (MPa) were tested using the printed cubes after post-treatment. Dry bulk density was calculated using the following equation:

$$\rho_{bulk} = \frac{m_d}{V_M},$$

where ρ_{bulk} is the dry bulk density (g/cm^3), m_d (g) is the weight of the cubic samples dried at room temperature for 24 h, and V_M is the volume (cm^3) as the whole of the cubic samples measured with a digital Vernier scale (Mitutoyo ABSOLUTE 500-197-20, Japan). The water absorption rate was calculated using the following equation:

$$W_a = \frac{m_w - m_d}{m_d} \times 100,$$

TABLE 2 | Physical characteristics of WSIA sampled monthly from N wastewater treatment facility located in Seoul during May to October 2020.

Sampling time	Water content (%)	Organic content (%)	Average of mean particle size (μm)
May	0.3 (± 0.1)	0.6	91.3 (± 0.8)
June	0.43 (± 0.12)	0.1	36.7 (± 0.1)
July	0.33 (± 0.06)	0.4	46.2 (± 0.4)
August	0.37 (± 0.06)	0.6	40.8 (± 0.0)
September	0.27 (± 0.06)	0.5	45.2 (± 1.4)
October	0.23 (± 0.06)	0.54	47.5 (± 0.3)
Average	0.32 (± 0.1)	0.45 (± 0.17)	51.3 (± 18.8)

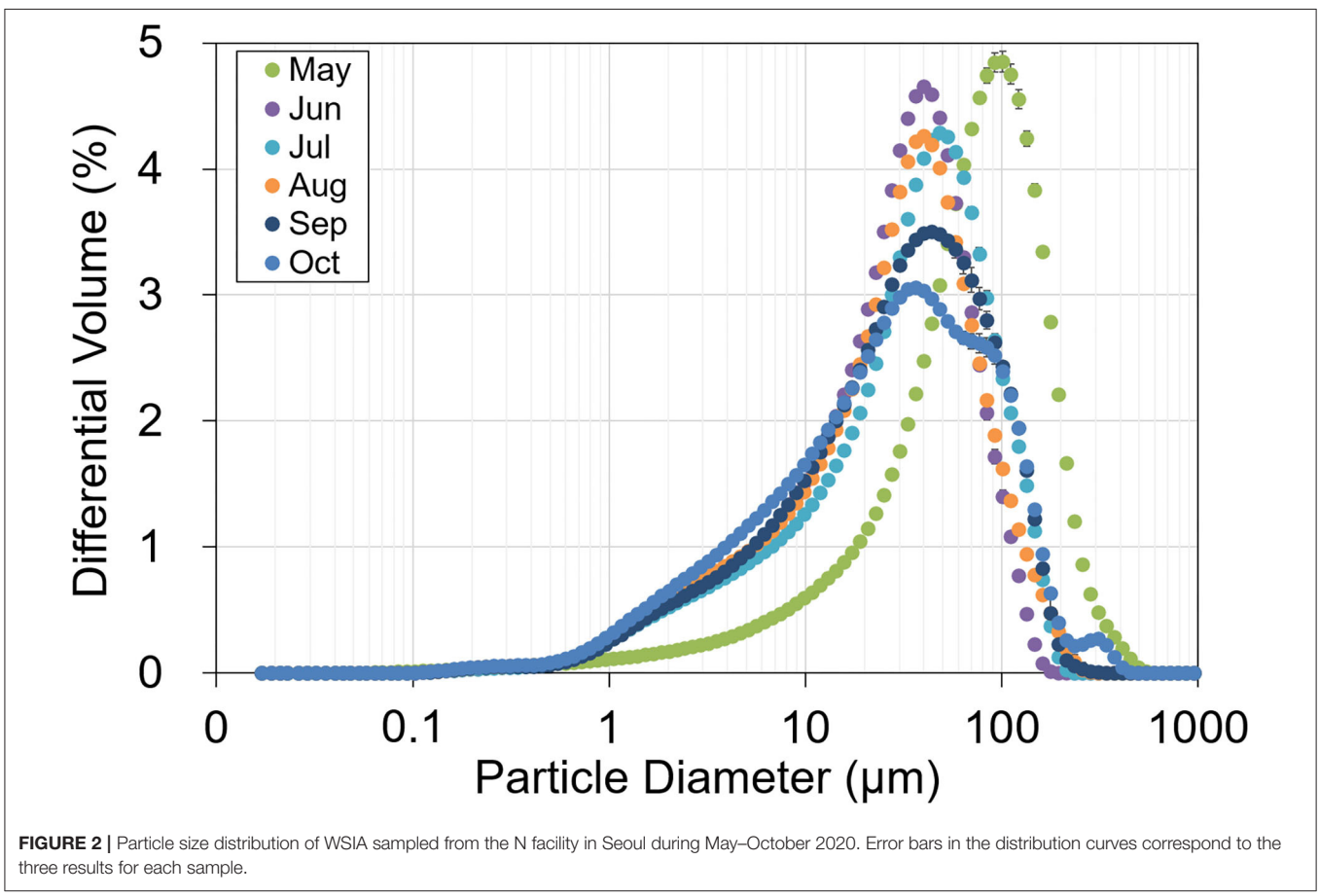

FIGURE 2 | Particle size distribution of WSIA sampled from the N facility in Seoul during May–October 2020. Error bars in the distribution curves correspond to the three results for each sample.

where W_a is the water absorption rate (%) and m_w is the weight of the cubic samples after they are extracted from the immersion liquid (water) and the excess water on the surface is removed. To measure m_w, the cubes were submerged in the immersion liquid for 1 h. The compressive strength of the post-treated cubic samples was measured in the Z-direction after 7 d. The Z-direction is a layer stacking direction of the Universal Testing Machine (UTM, INSTRON) with a maximum load of 50 kN under load control at a rate of 0.04 kN/s or 10 mm/min. Three functional parameter tests (density, water absorption rate, and compressive strength) were performed for each incinerated ash mixing ratio scenario (0, 25, 50%) and five post-treatment options.

For the environmental assessment of the printed products, we analyzed six heavy metals (Cr^{+6}, Cu, Cd, Pb, As, and Hg) that leached from the cubic samples and followed the Korean Official Wastes Test Method (Ministry of Environment (MOE), 2017). Samples were pretreated with an acid solution, the emission line was subsequently detected, and the intensities of Cr^{+6}, Cu, Cd, Pb, and As were measured using ICP-OES (Optima 8300, PerkinElmer, UK). Mercury (Hg) was quantified using the generated mercury vapor at a wavelength of 253.7 nm via an atomic absorption spectrophotometer (AAS) (FIMS 400, PerkinElmer, UK).

RESULTS AND DISCUSSION

Stability Characteristics of WSIA

The water content, organic content, and particle size results of the WSIA samples are summarized in **Table 2**. Due to the high temperature (typically >800°C) of sludge incineration, water and organic contents were <1%. Organic content measurements met the Korean standard of <5% as specified by the Waste Control Act. The monthly average particle size ranged between 37 and 48 μm except for the sample (91 μm) collected in May. In addition, more than 75% of the particle sizes ranged between 2 and 100 μm. Overall, the average size was ∼51 μm, and the particle size distributions for each sample during May to October are shown in **Figure 2**.

Monthly oxide compound ratios by weight are shown in **Figure 3** with averages presented in **Table 3**. The major compounds (>20% each) were SiO_2 (29.6%), Al_2O_3 (24.7%), P_2O_5 (21%), Fe_2O_3 (8.8%), and CaO (7.3%). In addition, as shown in **Figure 4**, Si, Al, P, Fe, and Ca were qualitatively measured using XRD (**Figure 4**). During August and September 2020, SiO_2 and Al_2O_3 concentrations increased and P_2O_5 and CaO concentrations decreased (**Figure 3**). Overall, the fluctuation in the chemical composition of the incineration ash was minimal during the six-month experiment.

Characterization of the physical and chemical properties of WSIA is important for determining the potential

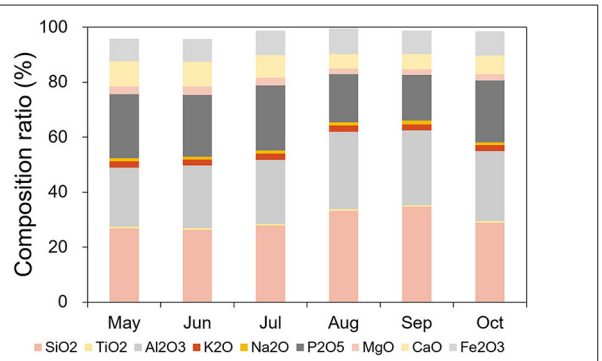

FIGURE 3 | Ratio of WSIA in oxide compounds sampled from the N facility in Seoul during May–October 2020.

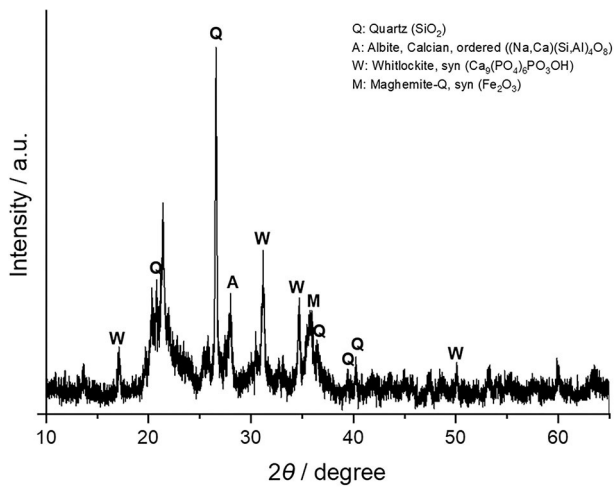

FIGURE 4 | XRD patterns of WSIA sampled in May.

TABLE 3 | Chemical (oxide compounds) composition ratio (%) of WSIA from N facility in Seoul, South Korea.

	SiO_2	TiO_2	Al_2O_3	K_2O	Na_2O	P_2O_5	MgO	CaO	Fe_2O_3
This study*	29.6 (±3.5)	0.6 (±0.0)	24.7 (±2.6)	2.2 (±0.1)	1.1 (±0.1)	21.0 (±3.1)	2.5 (±0.4)	7.3 (1.8)	8.8 (±0.6)
Lee and Lim (2009)	27.3	1.1	13.5	1.8	1.6	17.6	3.6	9.5	8.8
Lee (2015)	16.0	-	12.0	1.9	2.0	14.0	1.7	15.4	21.2
Shin et al. (2004)	53.3	0.9	17.4	3.1	2.9	0.5	3.0	4.0	8.0

**Loss on ignition (LOI) was 0.45 ± 0.17%.*

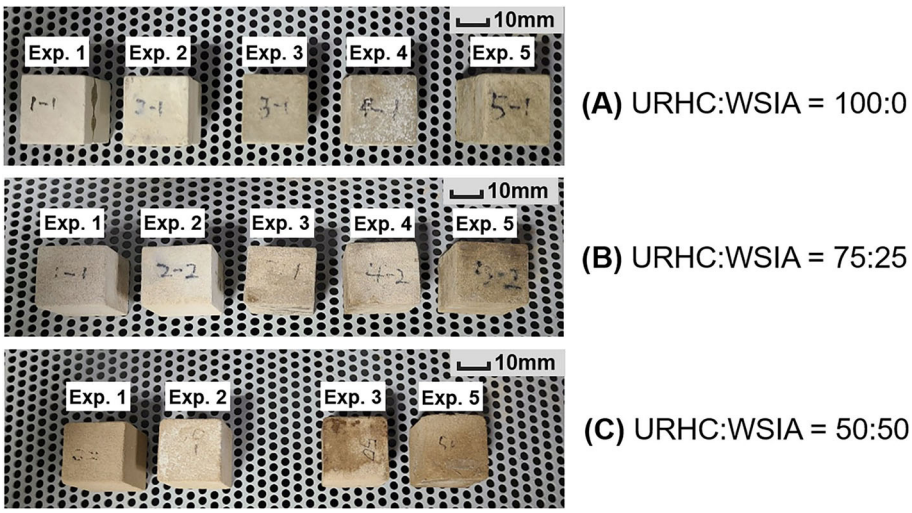

FIGURE 5 | Three-dimensional printed specimens comprising URHC mixed with WSIA in different weight ratios: **(A)** 0%, **(B)** 25%, and **(C)** 50%.

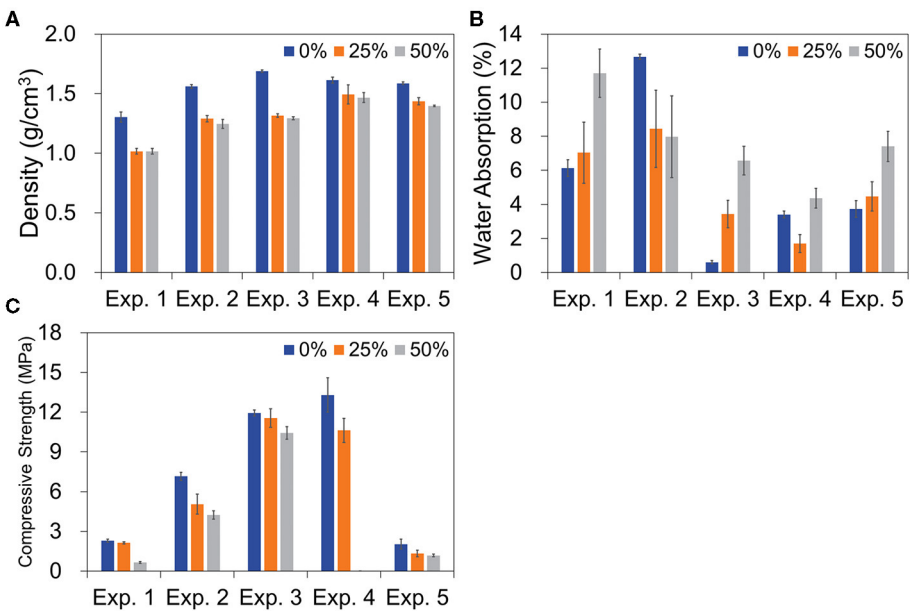

FIGURE 6 | Physical characteristics of 3D printed cubic specimens with varying WSIA mixing ratios (0, 25, and 50%) in different post-treatments (Experiments 1–5): **(A)** volumetric density, **(B)** water absorption, and **(C)** compressive strength.

of ash as a base material and value-added resource in 3D printing. Depending on the location of the WSIA generation, characteristics could differ due to influent properties, chemical use in the treatment processes, and other wastewater treatment process variables (Park et al., 2008; Kim and Lee, 2016). The composition ratios of oxide compounds from current and previous studies are provided in **Table 3**; however, previous studies mostly investigate only a single sample (Shin et al., 2004; Lee and Lim, 2009; Lee, 2015). The current study includes monitoring of ash characteristics to confirm composition stability and reliability as a recycled resource.

Optimal Ratio of the Composite Mixture of WSIA + URHC

Figure 5 shows the 3D printed cubic specimens produced using the composite powder materials, which have been prepared using URHC and different ratios of WSIA by weight with and without post-treatment in different solutions (Experiments 1–5). **Figure 6** shows the comparison among Experiment 1

TABLE 4 | Comparisons of 3D printing outputs on strength applied with different materials and curing conditions.

3D printing materials	Mixed conditions	"Green" strength (MPa, Z-direction)	Curing conditions (mixture and curing temperature)	Compressive strength (MPa, Z-direction)	References
Slag+silicate-based activator+fine sand	Not informed	0.76	Anhydrous sodium metasilicate solution; $SiO_2/Na_2O = 2\sim3.2$ [71.4% w/w]+ NaOH [28.6% w/w] solutions, 60°C	15.7–26	Xia and Sanjayan, 2016; Nematollahi et al., 2019
Calcium sulfate hemihydrate (plaster-based powder)	$CaSO_4$ $1/2H_2O$ [1]	0.61	Anhydrous sodium metasilicate solution, 60°C	-	Xia and Sanjayan, 2016
Slag+low calcium fly ash+silicate-based activator	Slag+fly ash [0.7]+silica-based activator [0.3]	0.24–0.76	$SiO_2/Na_2O = 0.9\sim3.22$ [71.4∼100% w/w]+ NaOH [28.6∼0% w/w], 60°C	6.1–26.5	Xia et al., 2019
Fly ash+ground granulated blast furnace slag	Not informed	1.46	$SiO_2/Na_2O = 1$, $Na_2SiO_3/NaOH = 1$ (1M NaOH), 70°C	7.1	Park et al., 2018
URHC+wastewater sludge incinerated ash	URHC [0.5–0.75]+WSIA [0.5-0.25]	0.65–2.13	$SiO_2/Na_2O = 0.95$ or $Na_2SiO_3/NaOH = 3$ (3M NaOH), 70°C	10.4–11.6	This study
URHC	URHC [1]	2.3	$SiO_2/Na_2O = 0.95$ or $Na_2SiO_3/NaOH = 3$ (3M NaOH), 70°C	11.9–13.3	This study

TABLE 5 | Heavy metal contents of the 3D printed cubic specimen in different post-treatments (Experiments 1–5).

Exp.	Heavy metal content (mg/L)					
	Cr^{6+}	Cu	Cd	Pb	As	Hg
1	0.15	0.013	N.D.	N.D.	N.D.	N.D.
2	0.04	0.010	N.D.	N.D.	N.D.	N.D.
3	0.06	0.018	N.D.	N.D.	N.D.	N.D.
4	0.08	0.010	N.D.	N.D.	N.D.	N.D.
5	0.13	0.019	N.D.	N.D.	N.D.	N.D.

[the control experiment without post-treatment referred to as the "green" sample in previous studies (Nematollahi et al., 2019)], Experiment 2 (post-treatment with the immersion liquid of water), Experiment 3 (using alkali solution used as a commercially available surface hardener), Experiment 4 (employing an alkaline solution of Na_2SiO_3 and NaOH), and Experiment 5 (utilizing PDMS solution). The results show an increase in volumetric densities in Experiments 2–5. An increase in water absorption is shown in Experiment 2, and a decrease is observed in Experiments 3–5. Increases in compressive strength of the water and alkali solutions are observed in Experiments 2–4, and no further enhancement of the PDMS solution is shown in Experiment 5. Moreover, we confirm that an increase in the WSIA mixing ratios decreases the volumetric density and compressive strength in Experiments 3–5 while increasing the water absorption. For the 50% WSIA scenario in Experiment 4, the cubic specimen broke during curing in the post-treating medium; this was possibly due to an internal swelling that occurred due to an increase in the ash particles. In addition, the compressive strength may have been <0.5 MPa; however, we were not able to measure this characteristic (**Figures 5**, **6**). A commercially available Sika solution (Experiment 3) did not provide a detailed composition description, such as a modulus ratio of SiO_2/Na_2O and a weight percentage of Na_2O and SiO_2. Compared with the post-treatment solution of Experiment 4, alkaline reactions at a pH between 11 and 12 likely resulted in a significant curing effect; this led to a sharp drop in the strength of the 50% WSIA mixture (**Figure 6C**). The increased compressive strength after immersion in the sodium silicate curing medium (Experiments 3 and 4) could be attributed to available silicates penetrating the printed cube pores, thereby forming calcium silicate hydrate (C-S-H) and sodium aluminosilicate hydrate (N-A-S-H). These would be formed via geopolymerization among silicate, aluminate, and calcium hydroxide in the curing medium and the composite mixture of WSIA and URHC (Duxson et al., 2007). Based on the results, it is suggested that the optimal mixing ratio of WSIA with alkaline post-treating solutions is ∼25%. The physical characteristics of water absorption (1.7–3.4%) and compressive strength (10.6–11.6) in Experiments 3 and 4 containing 25% WSIA are in agreement with the Korean

Industrial Standards (2019); for a decorative concrete block, these standards recommend a compressive strength of >7.8 MPa and water absorption of <20%.

Previous studies also use industrial wastes, such as slag and fly ash, as materials for BJ3DP with different ratios and mixed them with other types of alkali-activated materials, such as anhydrous sodium silicate and sand (Xia and Sanjayan, 2016; Park et al., 2018; Nematollahi et al., 2019). As alkali-activation of the industrial wastes containing alumina and silica promote geopolymerization (Nematollahi et al., 2015), the major components of SiO_2 (29.6%) and Al_2O_3 (24.7%) in WSIA work in the same reaction along with BJ3DP, including post-processing. **Table 4** summarizes the key conditions of the experiments and the results of compressive strengths in previous and current studies. Numerous other options for different alkali-based materials from wastes and curing conditions should be tested in the future to improve mechanical properties and economics. A detailed economic analysis has not yet been performed in the literature.

Environmental Evaluation of 3D Printing Products Heavy Metal Concentrations

Wastewater influent may contain potentially hazardous substances, such as heavy metals, chlorinated hydrocarbons, and petroleum hydrocarbons. If these compounds are not effectively removed during wastewater treatment processes, they could accumulate in the sludge cakes and subsequently in the incinerated ash. Thus, the N wastewater facility in Seoul regularly performs hazardous substance monitoring. Test results from 6 years (2015–2020) of monitoring are provided in the **Supplementary Materials**. **Table 5** shows the concentrations of six heavy metal contents that are leached from the 3D printed cubic specimens from six experiments; Cr^{6+} and Cu were detected, but concentrations were significantly less than those in "designated waste" (<1.500 mg/L of Cr^{6+} and <3.00 mg/L of Cu) concentrations.

Outlook: Path Toward Sustainable Upcycle of WSIA

Currently, WSIA is defined as "industrial waste," which implies that only certified workers can extract and deliver it to the contracted destination; this hinders its sustainable use in various ways. This study provides a clear demonstration of the stability of the WSIA composition and hazardous substances. Moreover, optimal WSIA mixing ratios were studied. Based on these results, the waste discharger could report WSIA not as waste but as a resource following the new "Circular Resources Accreditation System." To achieve more sustainable upcycling of WSIA, the final products obtained using WSIA, such as decorative concrete or building exterior blocks, should be showcased first in the public domain.

CONCLUSIONS

This study monitored the physical and chemical characteristics of WSIA for 6 months to assess its stability as an upcycled resource for 3D printing. The major oxide compounds evaluated were SiO_2 (29.6%), Al_2O_3 (24.7%), P_2O_5 (21%), Fe_2O_3 (8.8%), and CaO (7.3%). The inorganic compounds in the WSIA were similar to those of slag, sand, and fly ash used in previous studies despite the different weight ratios of the compounds. The component concentration stability increases the upcycling potential of the waste. Thus, WSIA was employed as a geopolymer powder source for manufacturing 3D printing material that can be used with BJ3DP. It was determined that the optimized mixing ratio was ∼25% with URHC, which is a commercially available cement. Under the current physical properties of water absorption and compressive strength conditions, upcycled WSIA could be used in decorative concrete blocks according to the Korean Standard of KS F 4038: 2019. Further studies on the composite materials, which elucidate the effects of controlling the WSIA particle size and perform economic evaluations of the potential long-term curing period, should be conducted in the future.

DATA AVAILABILITY STATEMENT

The original contributions presented in the study are included in the article/**Supplementary Material**, further inquiries can be directed to the corresponding author.

AUTHOR CONTRIBUTIONS

DK designed the research project, collected, analyzed and interpreted the data, and wrote the paper. SK designed the analysis, helped with the data analysis, and contributed to writing and reviewing. K-MP performed the lab experiment and analysis. All authors contributed to the article and approved the submitted version.

FUNDING

This study has received funding from the Seoul Institute of Technology (SIT) (2020-AC-001 & 2021-AC-002).

ACKNOWLEDGMENTS

This study was supported by the Seoul Institute of Technology (SIT) research projects (2020-AC-001 & 2021-AC-002). The authors would like to thank Tae-Hwan Kim and Chan-Woo Kim in the Water Circulation Safety Bureau, Seoul Metropolitan Government to help obtaining the information of wastewater sludge statistics and incineration ash and connecting wastewater treatment facilities.

SUPPLEMENTARY MATERIAL

The Supplementary Material for this article can be found online at: https://www.frontiersin.org/articles/10.3389/frsus.2021.697265/full#supplementary-material

REFERENCES

Asadi-Eydivand, M., Solati-Hashjin, M., Shafiei, S. S., Mohammadi, S., Hafezi, M., and Abu Osman, N. A. (2016). Structure, properties, and *in vitro* behavior of heat-treated calcium sulfate scaffolds fabricated by 3D printing. *PLoS ONE* 11:e0151216. doi: 10.1371/journal.pone.0151216

ASTM International (2015). *Standard Terminology for Additive Manufacturing Technologies*. ASTM F42.

Bianchini, A., Bonfiglioli, L., Pellegrini, M., and Saccani, C. (2015). Sewage sludge drying process integration with a waste-to-energy power plant. *Waste Manag.* 42, 159–165. doi: 10.1016/j.wasman.2015.04.020

Burton, F. L., Tchobanoglous, G., Tsuchihashi, R., David Stensel, H., and Metcalf and Eddy Inc. (2014). *Wastewater Engineering: Treatment and Resource Recovery, 5th Edn*. New York, NY: McGraw-Hill.

Cieślik, B., and Konieczka, P. (2017). A review of phosphorus recovery methods at various steps of wastewater treatment and sewage sludge management. The concept of "no solid waste generation" and analytical methods. *J. Cleaner Prod.* 142, 1728–1740. doi: 10.1016/j.jclepro.2016.11.116

Davidovits, J. (1989). Geopolymers and geopolymeric materials. *J. Thermal Anal.* 35, 429–441. doi: 10.1007/BF01904446

Duxson, P., Fernández-Jiménez, A., Provis, J. L., Lukey, G. C., Palomo, A., and van Deventer, J. S. J. (2007). Geopolymer technology: the current state of the art. *J Mater Sci* 42, 2917–2933. doi: 10.1007/s10853-006-0637-z

Epstein, E., Taylor, J. M., and Chaney, R. L. (1976). Effects of sewage sludge and sludge compost applied to soil on some soil physical and chemical properties. *J. Environ. Qual.* 5, 422–426. doi: 10.2134/jeq1976.00472425000500040021x

EU (2020). EU Circular Economy Action Plan—A New Circular Economy Action Plan for a Cleaner and More Competitive Europe. Available online at: https://ec.europa.eu/environment/circular-economy/index_en.htm (accessed April 10, 2021).

Guerra-Rodríguez, S., Oulego, P., Rodríguez, E., Singh, D. N., and Rodríguez-Chueca, J. (2020). Towards the implementation of circular economy in the wastewater sector: challenges and opportunities. *Water* 12:1431. doi: 10.3390/w12051431

Kim, S., and Lee, W. (2016). Characterization of fly ash produced from a sewage sludge incineration facility in Korea. *J. Korean Soc. Environ. Eng.* 38, 96–99. doi: 10.4491/KSEE.2016.38.2.96

Korean Industrial Standards, KS F 4038. (2019). *Standard Specification for Decorate Concrete Block*. Korea: Korean Standards Association.

Lee, B.-J., Lee, J., and Kim, Y.-Y. (2017). Durability performance of concrete penetrated and coated by polydimethylsiloxane for penetrating water repellency. *Korea Concrete Inst.* 29, 607–613. doi: 10.4334/JKCI.2017.29.6.607

Lee, H. (2015). Development of application block using geobond and ash from sewage sludge incinerator II. *J. Korean Soc. Environ. Eng.* 37, 412–417. doi: 10.4491/KSEE.2015.37.7.412

Lee, I.-S., and Kang, H.-Y. (2016). A review on the direction of the framework act on resource circulation for establishing a resource circulation society. *Korean Inst. Resour. Recycl.* 25, 82–91. doi: 10.7844/kirr.2016.25.6.82

Lee, K.-H., and Lim, J.-H. (2009). Investigation of the mixing melting incineration treatment of sewage sludge and municipal solid waste cinder. *Appl. Chem.* 13, 285–288.

Lim, S., Buswell, R. A., Le, T. T., Austin, S. A., Gibb, A. G. F., and Thorpe, T. (2012). Developments in construction-scale additive manufacturing processes. *Autom. Constr.* 21, 262–268. doi: 10.1016/j.autcon.2011.06.010

Lynn, C. J., Dhir, R. K., and Ghataora, G. S. (2016). Sewage sludge ash characteristics and potential for use in bricks, tiles and glass ceramics. *Water Sci. Technol.* 74, 17–29. doi: 10.2166/wst.2016.040

Mayer, A., Haas, W., Wiedenhofer, D., Krausmann, F., Nuss, P., and Blengini, G. A. (2019). Measuring progress towards a circular economy: a monitoring framework for economy-wide material loop closing in the EU28. *J. Indus. Ecol.* 23, 62–76. doi: 10.1111/jiec.12809

Maynard, A. D. (2015). Navigating the fourth industrial revolution. *Nat. Nanotech* 10, 1005–1006. doi: 10.1038/nnano.2015.286

Ministry of Environment (2020). *Statistic of Sewerage, Korea*. MOE.

Ministry of Environment (MOE) (2017). *Korean Official Wastes Test Method, Korea*. MOE.

Murray, A., Skene, K., and Haynes, K. (2017). The circular economy: an interdisciplinary exploration of the concept and application in a global context. *J. Bus. Ethics* 140, 369–380. doi: 10.1007/s10551-015-2693-2

Nematollahi, B., Sanjayan, J., and Shaikh, F. U. A. (2015). Synthesis of heat and ambient cured one-part geopolymer mixes with different grades of sodium silicate. *Ceramics Int.* 41, 5696–5704. doi: 10.1016/j.ceramint.2014.12.154

Nematollahi, B., Xia, M., and Sanjayan, J. (2017). "Current progress of 3D concrete printing technologies," in *34th International Symposium on Automation and Robotics in Construction (ISARC 2017)* (Taipei). doi: 10.22260/ISARC2017/0035

Nematollahi, B., Xia, M., and Sanjayan, J. (2019). Post-processing methods to improve strength of particle-bed 3D printed geopolymer for digital construction applications. *Front. Mater.* 6:160. doi: 10.3389/fmats.2019.00160

Park, J.-M., Kim, M.-J., Kim, J.-P., Lee, S.-B., Kwon, O.-S., and Lee, S.-H. (2008). Concentration of heavy metals and PAHs in sewage sludge. *J. Korean Soc. Environ. Anal.* 11, 275–281.

Park, K.-M., Lee, J., and Lee, B.-C. (2018). Improvement in strength of 3D printed alkali-activated slag/fly ash paste. *J. Korea Concrete Inst.* 30, 641–648. doi: 10.4334/JKCI.2018.30.6.641

Park, S.-W., and Jang, C.-H. (2011). Characteristics of carbonized sludge for co-combustion in pulverized coal power plants. *Waste Manag.* 31, 523–529. doi: 10.1016/j.wasman.2010.10.009

Rezaee, F., Danesh, S., Tavakkolizadeh, M., and Mohammadi-Khatami, M. (2019). Investigating chemical, physical and mechanical properties of eco-cement produced using dry sewage sludge and traditional raw materials. *J. Clean. Prod.* 214, 749–757. doi: 10.1016/j.jclepro.2018.12.153

Salmenperä, H., Pitkänen, K., Kautto, P., and Saikku, L. (2021). Critical factors for enhancing the circular economy in waste management. *J. Clean. Prod.* 280:124339. doi: 10.1016/j.jclepro.2020.124339

Shin, D. Y., Han, S. M., Kim, K. N., and Lee, H. J. (2004). The properties of permeability and freeze-thaw resistance of water-permeable paving brick using wastes. *J. Korean Ceramic Soc.* 41, 210–215. doi: 10.4191/KCERS.2004.41.3.210

Tantawy, M. A., El-Roudi, A. M., Abdalla, E. M., and Abdelzaher, M. A. (2012). Evaluation of the pozzolanic activity of sewage sludge ash. *ISRN Chem. Eng.* 9:487037. doi: 10.5402/2012/487037

UN (2016). *The Sustainable Development Agenda.* Available online at: http://www.un.org/sustainabledevelopment/development-agenda/ (accessed September 25, 2015).

Wang, F., Lei, S., Ou, J., and Li, W. (2020). Effect of PDMS on the waterproofing performance and corrosion resistance of cement mortar. *Appl. Surf. Sci.* 507:145016. doi: 10.1016/j.apsusc.2019.145016

Wu, P., Wang, J., and Wang, X. (2016). A critical review of the use of 3-D printing in the construction industry. *Autom. Constr.* 68, 21–31. doi: 10.1016/j.autcon.2016.04.005

Xia, M., Nematollahi, B., and Sanjayan, J. (2019). Printability, accuracy and strength of geopolymer made using powder-based 3D printing for construction applications. *Autom. Constr.* 101, 179–189. doi: 10.1016/j.autcon.2019.01.013

Xia, M., and Sanjayan, J. (2016). Method of formulating geopolymer for 3D printing for construction applications. *Mater. Design* 110, 382–390. doi: 10.1016/j.matdes.2016.07.136

Xia, M., and Sanjayan, J. G. (2018). Methods of enhancing strength of geopolymer produced from powder-based 3D printing process. *Mater. Lett.* 227, 281–283. doi: 10.1016/j.matlet.2018.05.100

Conflict of Interest: The authors declare that the research was conducted in the absence of any commercial or financial relationships that could be construed as a potential conflict of interest.